

An efficient protocol of quantum walk in circuit QED

Jia-Qi Zhou, Qi-Ping Su,* and Chui-Ping Yang

Department of Physics, Hangzhou Normal University,

Hangzhou, Zhejiang 311121, China

(Dated: March 17, 2022)

Abstract

Implementation of discrete-time quantum walk (DTQW) with superconducting qubits is difficult since on-chip superconducting qubits cannot hop between lattice sites. We propose an efficient protocol for the implementation of DTQW in circuit quantum electrodynamics (QED), in which only $N + 1$ qutrits and N assistant cavities are needed for an N -step DTQW. The operation of each DTQW step is very quick because only resonant processes are adopted. The numerical simulations show that high-similarity DTQW with the number of step up to 20 is feasible with present-day circuit QED technique. This protocol can help to study properties and applications of large-step DTQW in experiments, which is important for the development of quantum computation and quantum simulation in circuit QED.

* sqp@hznu.edu.cn

I. INTRODUCTION

Circuit quantum electrodynamics (QED), composed of superconducting qubits and microwave resonators or cavities, has attracted substantial attention because of its controllability, integrability, ready fabrication and potential scalability [1–7] in quantum information and quantum computation. The strong coupling and ultrastrong coupling of a qubit with a microwave cavity in experiments have been reported [8, 9]. The level spacings of superconducting qubits can be rapidly adjusted ($1 \sim 3$ ns) [10–13], and their coherence time is improved rapidly [14–19]. The circuit QED is considered as one of the most feasible candidates for quantum computation and quantum simulation [6, 7].

Quantum walk is extension of the classical random walk, which has wide applications in quantum algorithms [20–22], quantum simulation [23–26], universal quantum computation [27–29], and so on [30, 31]. In the standard DTQW, there is a walker moving with respect to the state of a coin. The evolutions of the walker and the coin are characterized by a unitary operator $U = W \cdot C$. In each step of a 1-dimensional (1D) DTQW, at first, the coin with states $|0\rangle_c$ and $|1\rangle_c$ is tossed by the operator

$$C = \cos \theta |0\rangle_c \langle 0| + \sin \theta |0\rangle_c \langle 1| + \sin \theta |1\rangle_c \langle 0| - \cos \theta |1\rangle_c \langle 1|, \quad (1)$$

with $\theta \in (0, \pi/2)$, then the walker is shifted by

$$W = \sum_j |j+1\rangle \langle j| \otimes |0\rangle_c \langle 0| + |j-1\rangle \langle j| \otimes |1\rangle_c \langle 1|, \quad (2)$$

where the integer j represent sites of the walker in the 1D line. The implementations of DTQW have been achieved in several quantum systems, such as linear optics [22–24, 32–34], ion traps [35, 36], and neutral atom traps [37].

But it is not easy to implement DTQW in circuit QED. Unlike other systems, the superconducting qubits in circuit QED can not move. The encoding of states of the coin and the walker in superconducting qubits is difficult. There are only a few DTQW schemes in circuit QED. In [38, 39], the phase space of superposition states in a cavity is used to encode the walker’s position and a coupled qubit is used as the coin. Due to the adopted non-orthogonal states of the cavity and the limitation of the phase space, the generality and the scalability of this scheme are inevitable problems. In [40], a 1D DTQW scheme is proposed, in which a pair of superconducting qubits are used as a node and nearest-neighbor qubits are coupled



FIG. 1. (color online) Setup for implementation of DTQW in circuit QED, which consists of $N + 1$ qutrits and N cavities.

via tunable couplers. The walker moves in the 1D line of nodes and the coin is encoded by the position of the occupied qubit in each node. In this way, an N -step DTQW needs at least $4N + 2$ qubits and $4N + 1$ couplers.

In recent years, quantum information processing with qudits (d -level systems), including qutrits (i.e., $d = 3$), has been attracting increasing interest, since qudits (with $d > 2$) can be used to encode more information. For example, quantum information processing and tomography of nanoscale semiconductor devices were studied [41, 42]. In [43, 44], schemes for quantum state transfer of a qutrit in circuit QED were proposed.

In this paper, we propose an efficient and simple protocol for implementation of DTQW in circuit QED, in which only $N + 1$ qutrits (with 3 energy levels) and N cavities (i.e., the couplers) are needed for an N -step DTQW. Since only resonant processes are adopted, the operation of each DTQW step is very quick. With this protocol, arbitrary initial states of the coin can be prepared and arbitrary operation of the coin can be implemented easily. To estimate the implementation of this protocol and the effects of parameters, we numerically simulate the DTQW in a superconducting system with the number of step up to 20. It indicates that this protocol is feasible with the present circuit QED technology and can be used to implement a large-step DTQW. Because of the scalability and rapid improvement of circuit QED technology, this protocol can help to study properties and applications of large-step DTQW in experiments, which is important for the development of quantum information science.

II. A 1D DTQW PROTOCOL

As shown in Fig. 1, the setup consists of $N + 1$ qutrits (with energy levels $|g\rangle$, $|e\rangle$ and $|f\rangle$) and N cavities. All qutrits have the same energy levels and the frequency of cavities

(ω_c) is equal to the $|g\rangle \leftrightarrow |e\rangle$ transition frequency of the qutrits (ω_{eg}). The walker's position is represented by the position of the qutrit in a non-ground state (i.e., superposition state of $|e\rangle$ and $|f\rangle$), and the coin states $|0\rangle_c$ and $|1\rangle_c$ are represented by the states $|f\rangle$ and $|e\rangle$, respectively. In this case, arbitrary initial state of the coin can be prepared easily by applying corresponding pulses to the qutrits. Suppose all cavities are initially in the ground state $|0\rangle$ and decoupled with qutrits, the steps for the implementation of the DTQW are as follows.

Step I: Tossing the coin by applying a pulse (with the Rabi frequency Ω) to each qutrit. The frequency, duration, initial phase of the pulses are ω_{fe}, t_1, ϕ , respectively. In the interaction picture, the Hamiltonian for qutrits interacting with the pulses is

$$H_{I,1} = \sum_j \Omega (e^{i\phi} |e\rangle_j \langle f| + e^{-i\phi} |f\rangle_j \langle e|).$$

This Hamiltonian makes the following transformations for states of qutrit j ($j = 1, 2, 3, \dots, N+1$):

$$\begin{aligned} |g\rangle_j &\rightarrow |g\rangle_j, \\ |e\rangle_j &\rightarrow \cos(\Omega t_1) |e\rangle_j - i e^{-i\phi} \sin(\Omega t_1) |f\rangle_j, \\ |f\rangle_j &\rightarrow -i e^{i\phi} \sin(\Omega t_1) |e\rangle_j + \cos(\Omega t_1) |f\rangle_j. \end{aligned} \quad (3)$$

It shows that arbitrary unitary operator of the coin can be achieved by applying suitable pulses. If we set $t_1 = \theta/\Omega$ and $\phi = -\pi/2$, this operation of the coin is just that of $\sigma_z \cdot C$, where C is the coin operator in Eq. (1) and $\sigma_z = |0\rangle_c \langle 0| - |1\rangle_c \langle 1|$. The shift operation of the walker with respect to the coin state will be accomplished by the following two steps.

Step II: Coupling cavity j with the qutrit j (assuming the coupling strength $g_j = g$ with $j = 1, 2, 3, \dots, N$). The Hamiltonian in the interaction picture is

$$H_{I,2} = \sum_j g (a_j |e\rangle_j \langle g| + a_j^\dagger |g\rangle_j \langle e|).$$

After the evolution time $t_{II} = \pi/2g$, the transformations for the states of the qutrit j and the cavity j are:

$$\begin{aligned} |g\rangle_j |0\rangle_j &\rightarrow |g\rangle_j |0\rangle_j, \\ |e\rangle_j |0\rangle_j &\rightarrow -i |g\rangle_j |1\rangle_j, \\ |f\rangle_j |0\rangle_j &\rightarrow |f\rangle_j |0\rangle_j. \end{aligned} \quad (4)$$

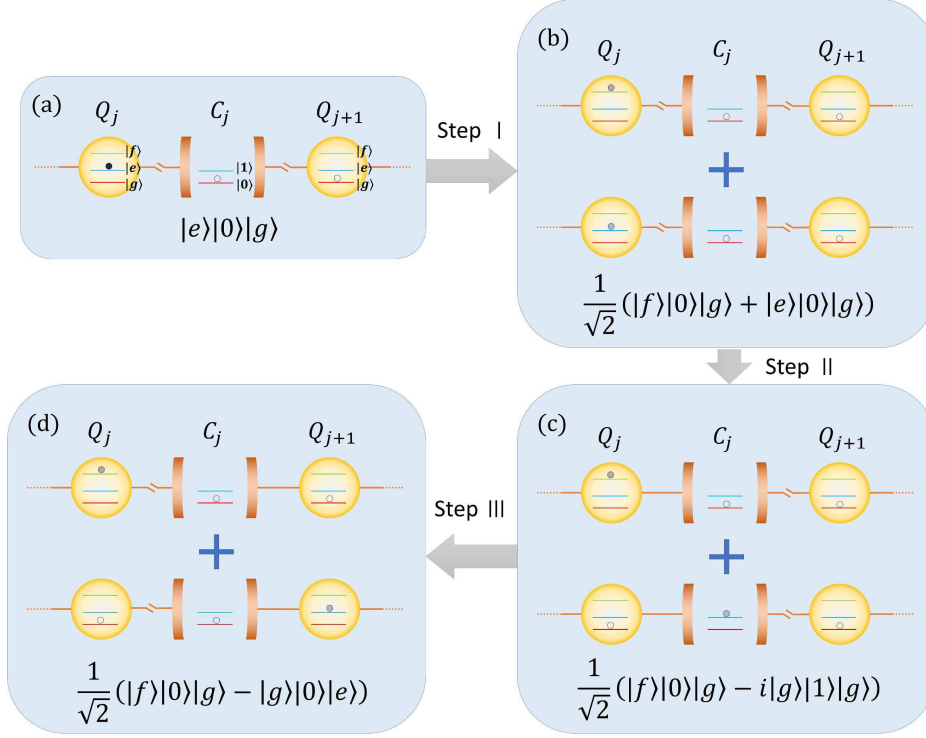


FIG. 2. (color online) Illustration of implementing steps of DTQW and state evolutions by assuming that energy level $|e\rangle$ of the qutrit j is initially occupied (i.e., initially the walker is at the position j and the coin state is $|1\rangle$). The small circles indicate the occupied energy levels. Hollow circles represent the occupation of ground states and the shade of solid circles represent the probability of the occupation of non-ground states. $\theta = \pi/4$ has been assumed for the coin operator C .

Step III: Decoupling cavity j from the qutrit j and coupling cavity j with the qutrit $j + 1$ (assuming the coupling strength $g'_j = \mu$ with $j = 1, 2, 3, \dots, N$). Now the Hamiltonian in the interaction picture becomes

$$H_{I,3} = \sum_j \mu (a_j |e\rangle_{j+1} \langle g| + a_j^\dagger |g\rangle_{j+1} \langle e|).$$

After the evolution time $t_{\text{III}} = \pi/2\mu$, the transformations for the states of the cavity j and the qutrit $j + 1$ are:

$$\begin{aligned} |0\rangle_j |g\rangle_{j+1} &\rightarrow |0\rangle_j |g\rangle_{j+1}, \\ |1\rangle_j |g\rangle_{j+1} &\rightarrow -i|0\rangle_j |e\rangle_{j+1}. \end{aligned} \tag{5}$$

If the walker is initially in position j (i.e., the qutrit j is excited), after the step II and step III, it will move into position $j + 1$ (i.e., the qutrit $j + 1$) with the coin state $|1\rangle_c$ ($|e\rangle_{j+1}$) or it will stay in position j (i.e., the qutrit j) with the coin state $|0\rangle_c$ ($|f\rangle_j$). This shift operation of the walker achieved in step II,III can be expressed as $W' \cdot \sigma_z$, where $W' = \sum_j (|j\rangle\langle j| \cdot |0\rangle_c\langle 0| + |j+1\rangle\langle j| \cdot |1\rangle_c\langle 1|)$. Note that W' is equivalent to the operator W in Eq.(2).

Now the standard DTQW operation $U' = W' \cdot C$ is achieved with the operational time $t = t_I + t_{II} + t_{III}$. In Fig. 2, the evolutions of the states of the qutrits j , $j + 1$ and the cavity j with steps I,II and III are demonstrated by assuming an initial state of $|j\rangle|1\rangle_c$ (i.e., $|e\rangle_j$). Repeating the step I,II,III by N times, an N -step 1D DTQW is realized.

III. POSSIBLE EXPERIMENTAL IMPLEMENTATION

In this section, we discuss the feasibility for the implementation of this DTQW protocol with DTQW steps up to 20 by numerical simulations. In all simulations, we set $\theta = \pi/4$ for the coin operator and assume that the walker starts from the qutrit 1. By considering

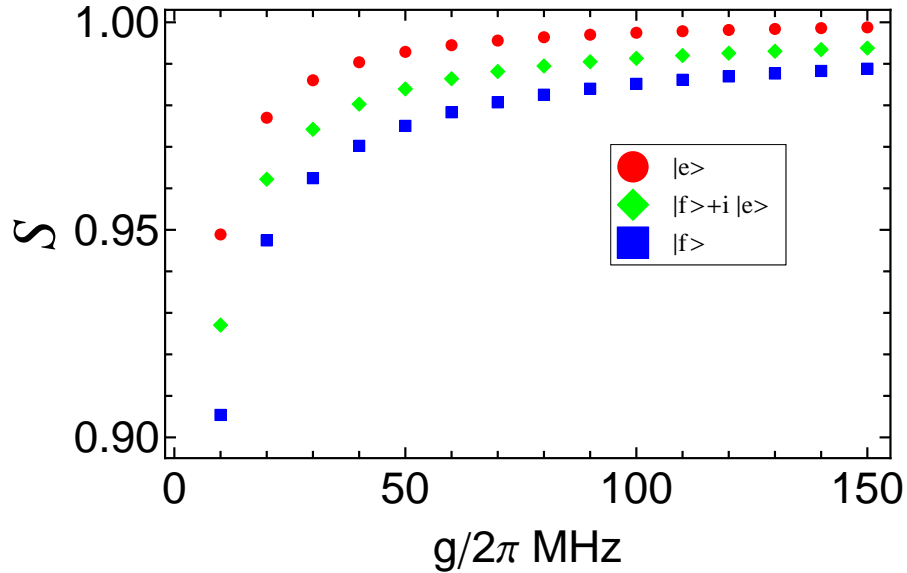


FIG. 3. (color online) Similarity versus $g/2\pi$ are plotted respectively for initial states of the coin $|0\rangle_c$, $|1\rangle_c$, $(|0\rangle_c + i|1\rangle_c)/\sqrt{2}$, with $N = 10$ and $\Omega/2\pi = 100$ MHz.

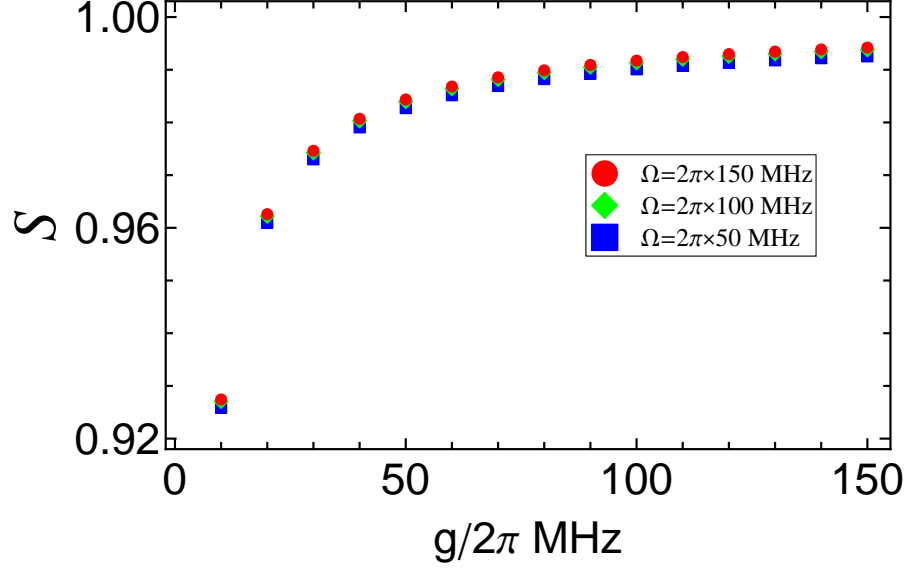


FIG. 4. (color online) Similarity versus $g/2\pi$ are plotted respectively for $\Omega/2\pi = 50, 100, 150$ MHz, with $N = 10$ and the initial state of the coin $(|0\rangle_c + i|1\rangle_c)/\sqrt{2}$.

dissipation and dephasing, the evolving of the system is determined by the master equation

$$\begin{aligned}
\frac{d\rho}{dt} = & -i[H_{I,k}, \rho] + \sum_j \kappa_{a_j} \mathcal{L}[a_j] \\
& + \sum_j \gamma_{ef,j} \mathcal{L}[\sigma_{ef,j}^-] + \gamma_{gf,j} \mathcal{L}[\sigma_{gf,j}^-] + \gamma_{ge,j} \mathcal{L}[\sigma_{ge,j}^-] \\
& + \sum_j \gamma_{e\varphi,j} \mathcal{L}[\sigma_{ee,j}] + \gamma_{f\varphi,j} \mathcal{L}[\sigma_{ff,j}], \tag{6}
\end{aligned}$$

where $\mathcal{L}[\Lambda] = \Lambda\rho\Lambda^\dagger - \Lambda^\dagger\Lambda\rho/2 - \rho\Lambda^\dagger\Lambda/2$ (with $\Lambda = a_j, \sigma_{ef,j}^-, \sigma_{gf,j}^-, \sigma_{ge,j}^-, \sigma_{ee,j}, \sigma_{ff,j}$), $\sigma_{ef,j}^- = |e\rangle_j \langle f|$, $\sigma_{gf,j}^- = |g\rangle_j \langle f|$, $\sigma_{ge,j}^- = |g\rangle_j \langle e|$, $\sigma_{ee,j} = |e\rangle_j \langle e|$, and $\sigma_{ff,j} = |f\rangle_j \langle f|$; κ_{a_j} is the decay rate of cavity j ; $\gamma_{ef,j}$ ($\gamma_{gf,j}$) is the energy relaxation rate for the level $|f\rangle$ associated with the decay path $|f\rangle \rightarrow |e\rangle$ ($|f\rangle \rightarrow |g\rangle$) of qutrit j ; $\gamma_{ge,j}$ is the energy relaxation rate of the level $|e\rangle$; and $\gamma_{f\varphi,j}$ ($\gamma_{e\varphi,j}$) is the dephasing rate of the level $|f\rangle$ ($|e\rangle$) of qutrit j .

In actual experiments, the probability distribution $P(j)$ of the walker is always easy to measure. So we calculate the similarity $S = \left(\sum_j \sqrt{P_{me}(j)P_{id}(j)}\right)^2$ to compare the $P_{me}(j)$ from the master equation (6) with the ideal $P_{id}(j)$ of the standard DTQW. In numerical simulations, flux qutrits are adopted and the decoherence parameters used are: (i) $\gamma_{e\varphi,j}^{-1} = 5 \mu\text{s}$, $\gamma_{f\varphi,j}^{-1} = 5 \mu\text{s}$; (ii) $\gamma_{ge,j}^{-1} = 10 \mu\text{s}$, $\gamma_{ef,j}^{-1} = 10 \mu\text{s}$, $\gamma_{gf,j}^{-1} = 10 \mu\text{s}$ [45–49], and (iii) $\kappa_{a_j}^{-1} = 10 \mu\text{s}$ [50, 51]. We denote this set of the decoherence parameters as T and the above choice of T as T_0 . For simplicity, we will set the coupling strengths $g_j = g'_j = g$. We will study

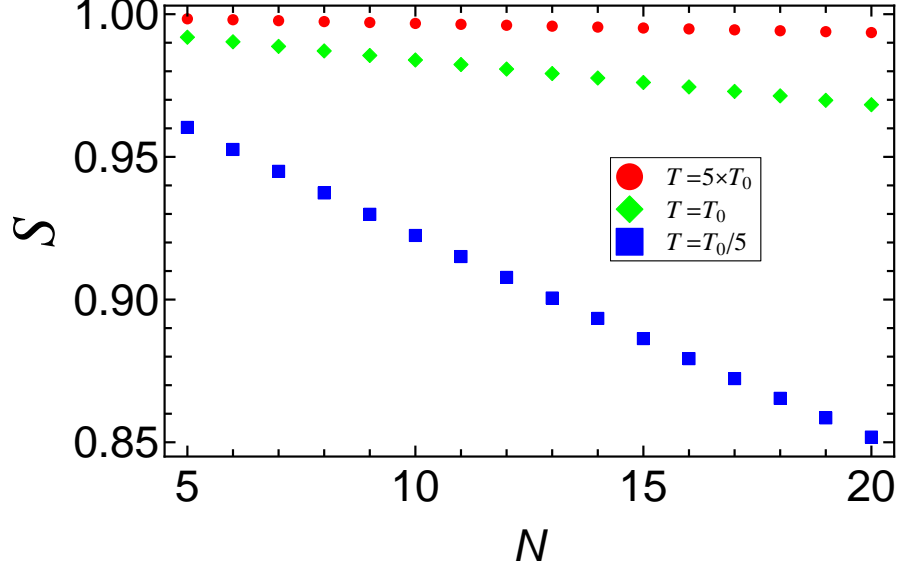


FIG. 5. (color online) Similarity versus number of step N are plotted respectively for $T = 5T_0, T_0, T_0/5$, with $g/2\pi = 50$ MHz, $\Omega/2\pi = 100$ MHz and the initial state of the coin $(|0\rangle_c + i|1\rangle_c)/\sqrt{2}$.

the effects of the coupling strength g , Rabi frequency Ω , initial state of the coin $|\phi_{c0}\rangle$, the number of DTQW steps N and the decoherence time set T on the similarity S .

In Fig. 3, the similarity versus $g/2\pi$ is plotted respectively for $|\phi_{c0}\rangle = |0\rangle_c, |1\rangle_c$ and $(|0\rangle_c + i|1\rangle_c)/\sqrt{2}$ (i.e., $|f\rangle, |e\rangle$ and $(|f\rangle + i|e\rangle)/\sqrt{2}$), with $N = 10$ and $\Omega/2\pi = 100$ MHz [52]. It is shown that different initial states of the coin lead to different similarities. Since each initial state of the coin is a superposition of $|0\rangle_c$ and $|1\rangle_c$ (i.e., $|f\rangle$ and $|e\rangle$), the lowest similarity for all initial states should be that with the initial state $|0\rangle_c$ (i.e., $|f\rangle$). As $g/2\pi = 50$ MHz, it shows that the similarity S is larger than 0.975 for an arbitrary initial state of the coin in the 10-step DTQW. Moreover, the similarity increases with the increasing of g as expected. It is shown that high similarity of this protocol can be achieved with present technology of circuit QED.

In Fig. 4, similarity versus $g/2\pi$ are plotted respectively for $\Omega/2\pi = 50, 100, 150$ MHz, with $N = 10$ and $|\phi_{c0}\rangle = (|0\rangle_c + i|1\rangle_c)/\sqrt{2}$. It shows that the similarity is not sensitive to the Rabi frequency Ω .

In Fig. 5, similarity versus number of step N are plotted respectively for $T = 5T_0, T_0, T_0/5$, with $g/2\pi = 50$ MHz, $\Omega/2\pi = 100$ MHz and $|\phi_{c0}\rangle = (|0\rangle_c + i|1\rangle_c)/\sqrt{2}$. It indicates that similarity decreases with the increasing of N and with the decreasing of T as expected. For

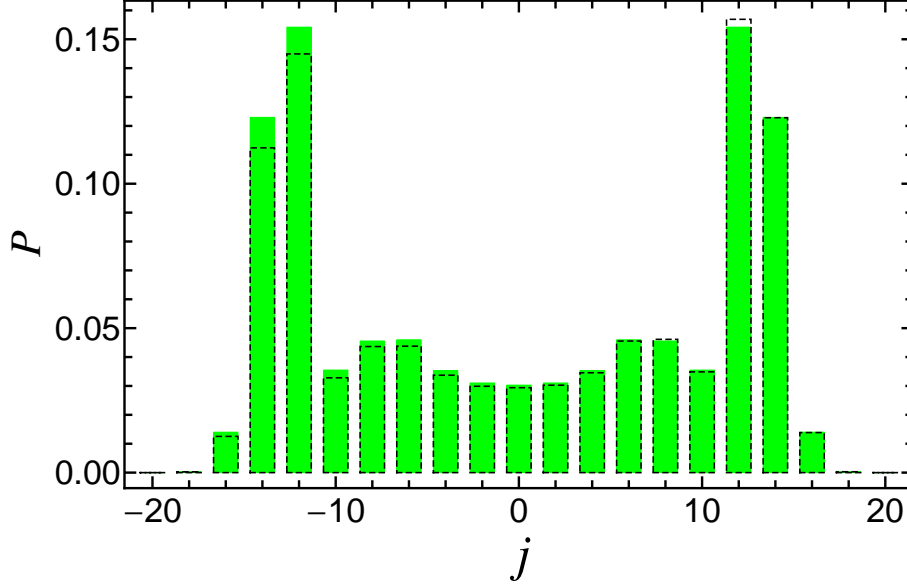


FIG. 6. (color online) Probability distribution of the DTQW from the numerical simulation (dashed bars) compared with that of the ideal DTQW (green bars), with $N = 20$, $T = T_0$, $g/2\pi = 50$ MHz, $\Omega/2\pi = 100$ MHz and the initial state of the coin $(|0\rangle_c + i|1\rangle_c)/\sqrt{2}$.

larger T , similarity decreases more slowly with the increasing of the step N . For larger N , similarity is more sensitive to the variance of T . For $N = 20$, we obtain similarity $S \sim 0.993, 0.968, 0.852$ with $T = 5T_0, T_0, T_0/5$, respectively. If the coherent times of the devices are not very small, high similarity for a large step DTQW can still be achieved with this DTQW protocol in circuit QED.

In Fig. 6, we show the probability distribution of the DTQW from the numerical simulation and that of the ideal DTQW, with $N = 20$, $T = T_0$, $g/2\pi = 50$ MHz, $\Omega/2\pi = 100$ MHz and the initial state of the coin $(|0\rangle_c + i|1\rangle_c)/\sqrt{2}$. In this case, the similarity S is ~ 0.968 and the numerical simulation indicates that probability distribution of the DTQW implemented in circuit QED with number of steps up to 20 still meets well with that of ideal DTQW.

IV. CONCLUSIONS

We have presented a protocol for implementing standard DTQW in circuit QED. The protocol is simple and efficient, only $N + 1$ qutrits and N assistant cavities are needed for an N -step DTQW and the operational time for each step is rather short due to the adoption of resonant processes. With this protocol, arbitrary initial states of the coin can

be prepared and arbitrary operation of the coin can be implemented easily, which is necessary for the general researches and applications of DTQW. The numerical simulations prove that high-similarity DTQW with $N \leq 20$ is feasible with present-day circuit QED technique. This DTQW protocol is quite general and can be extended to implement multi-dimensional DTQW in circuit QED, which is important in the quantum computation and quantum simulation.

ACKNOWLEDGMENTS

This work was supported in part by the NKRD of China (Grant No. 2016YFA0301802), the National Natural Science Foundation of China under Grant Nos. [11504075, 11074062, 11374083].

-
- [1] C. P. Yang, S. I. Chu and S. Y. Han, Possible realization of entanglement, logical gates, and quantum-information transfer with superconducting-quantum-interference-device qubits in cavity QED, *Phys. Rev. A* **67**, 042311 (2003).
 - [2] J. Q. You and F. Nori, Quantum information processing with superconducting qubits in a microwave field, *Phys. Rev. B* **68**, 064509 (2003).
 - [3] A. Blais, R. Huang, A. Wallra, S. Girvin, and R. Schoelkopf, Cavity quantum electrodynamics for superconducting electrical circuits: An architecture for quantum computation, *Phys. Rev. A* **69**, 062320 (2004).
 - [4] J. Q. You and F. Nori, Superconducting circuits and quantum information, *Phys. Today* **58**(11), 42 (2005).
 - [5] J. Q. You and F. Nori, Atomic physics and quantum optics using superconducting circuits, *Nature* **474**, 589 (2011).
 - [6] I. Buluta, S. Ashhab, and F. Nori, Natural and artificial atoms for quantum computation, *Rep. Prog. Phys.* **74**, 104401 (2011).
 - [7] Z. L. Xiang, S. Ashhab, J. Q. You, and F. Nori, Hybrid quantum circuits: Superconducting circuits interacting with other quantum systems, *Rev. Mod. Phys.* **85**, 623 (2013).

- [8] A. Wallraff, D. I. Schuster, A. Blais, L. Frunzio, R. S. Huang, J. Majer, S. Kumar, S. M. Girvin, and R. J. Schoelkopf, Strong coupling of a single photon to a superconducting qubit using circuit quantum electrodynamics, *Nature* **431**, 162 (2004).
- [9] T. Niemczyk, F. Deppe, H. Huebl, E. P. Menzel, F. Hocke, M. J. Schwarz, J. J. Garcia-Ripoll, D. Zueco, T. Hummer, E. Solano, A. Marx, and R. Gross, Circuit quantum electrodynamics in the ultrastrong-coupling regime, *Nat. Phys.* **6**, 772 (2010).
- [10] R. Barends, J. Kelly, A. Megrant, D. Sank, E. Jeffrey, Y. Y. Chen, Y. Yin, B. Chiaro, J. Mutus, C. Neill, P. O'Malley, P. Roushan, J. Wenner, T. C. White, A. N. Cleland, and J. M. Martinis, Coherent Josephson qubit suitable for scalable quantum integrated circuits, *Phys. Rev. Lett.* **111**, 080502 (2013).
- [11] M. Neeley, M. Ansmann, R. C. Bialczak, M. Hofheinz, N. Katz, E. Lucero, A. O'Connell, H. Wang, A. N. Cleland, and J. M. Martinis, Process tomography of quantum memory in a Josephson-phase qubit coupled to a two-level state, *Nat. Phys.* **4**, 523 (2008).
- [12] P. J. Leek, S. Filipp, P. Maurer, M. Baur, R. Bianchetti, J. M. Fink, M. Goppl, L. Steffen, and A. Wallraff, Using sideband transitions for two-qubit operations in superconducting circuits, *Phys. Rev. B* **79**, 180511(R) (2009).
- [13] J. D. Strand, M. Ware, F. Beaudoin, T. A. Ohki, B. R. Johnson, A. Blais, and B. L. T. Plourde, First-order sideband transitions with flux-driven asymmetric transmon qubits, *Phys. Rev. B* **87**, 220505(R) (2013).
- [14] J. M. Chow, J. M. Gambetta, A. D. Croles, S. T. Merkel, J. A. Smolin, C. Rigetti, S. Poletto, G. A. Keefe, M. B. Rothwell, J. R. Rozen, M. B. Ketchen, and M. Steffen, Universal Quantum Gate Set Approaching Fault-Tolerant Thresholds with Superconducting Qubits, *Phys. Rev. Lett.* **109**, 060501 (2012).
- [15] J. B. Chang, M. R. Vissers, A. D. Croles, M. Sandberg, J. Gao, D. W. Abraham, J. M. Chow, J. M. Gambetta, M. B. Rothwell, G. A. Keefe, M. Steffen, and D. P. Pappas, Improved superconducting qubit coherence using titanium nitride, *Appl. Phys. Lett.* **103**, 012602 (2013).
- [16] R. Barends, J. Kelly, A. Megrant, D. Sank, E. Jeffrey, Y. Chen, Y. Yin, B. Chiaro, J. Mutus, C. Neill, P. O'Malley, P. Roushan, J. Wenner, T. C. White, A. N. Cleland, and J. M. Martinis, Coherent Josephson Qubit Suitable for Scalable Quantum Integrated Circuits, *Phys. Rev. Lett.* **111**, 080502 (2013).

- [17] J. M. Chow, J. M. Gambetta, E. Magesan, D. W. Abraham, A. W. Cross, B. R. Johnson, N. A. Masluk, C. A. Ryan, J. A. Smolin, S. J. Srinivasan, and M. Steffen, Implementing a strand of a scalable fault-tolerant quantum computing fabric, *Nat. Commun.* **5**, 4015 (2014).
- [18] Y. Chen, C. Neill, P. Roushan, N. Leung, M. Fang, R. Barends, J. Kelly, B. Campbell, Z. Chen, B. Chiaro, A. Dunsworth, E. Jeffrey, A. Megrant, J. Y. Mutus, P. J. J. O’Malley, C. M. Quintana, D. Sank, A. Vainsencher, J. Wenner, T. C. White, M. R. Geller, A. N. Cleland, and J. M. Martinis, Qubit Architecture with High Coherence and Fast Tunable Coupling, *Phys. Rev. Lett.* **113**, 220502 (2014).
- [19] M. Stern, G. Catelani, Y. Kubo, C. Grezes, A. Bienfait, D. Vion, D. Esteve, and P. Bertet, Flux Qubits with Long Coherence Times for Hybrid Quantum Circuits, *Phys. Rev. Lett.* **113**, 123601 (2014).
- [20] S. Neil, K. Julia, and W. K. Birgitta, Quantum random-walk search algorithm, *Phys. Rev. A* **67**, 052307(2003).
- [21] C. Di Franco, M. Mc Gettrick, and Th. Busch, Mimicking the probability distribution of a two-dimensional Grover walk with a single-qubit coin, *Phys. Rev. Lett.* **106**, 080502 (2011).
- [22] Y. C. Jeong, C. Di Franco, H. T. Lim, M. S. Kim, and Y. H. Kim, Experimental realization of a delayed-choice quantum walk, *Nat. Comm.* **4**, 2471, (2013).
- [23] A. Crespi, R. Osellame, R. Ramponi, V. Giovannetti, R. Fazio, L. Sansoni, F. De Nicola, F. Sciarrino, and P. Mataloni, Anderson localization of entangled photons in an integrated quantum walk, *Nat. Photon.* **7**, 322 (2013).
- [24] X. Zhan, L. Xiao, Z. H. Bian, K. K. Wang, X. Z. Qiu, B. C. Sanders, W. Yi, and P. Xue, Detecting Topological Invariants in Nonunitary Discrete-Time Quantum Walks, *Phys. Rev. Lett.* **119**, 130501 (2017).
- [25] A. Peruzzo, M. Lobino, J. C. F. Mathews, N. Matsuda, A. Politi, K. Poulios, X. Q. Zhou, Y. Lahini, N. Ismail, K. Worhoff, Y. Bromberg, Y. Silberberg, M. G. Thompson, and J. L. O’Brien, Quantum walks of correlated photons, *Science* **329**, 1500 (2010).
- [26] T. Kitagawa, M. S. Rudner, E. Berg, and E. Demler, Exploring topological phases with quantum walk, *Phys. Rev. A* **82**, 033429 (2010).
- [27] A. M. Childs, Universal computation by quantum walk, *Phys. Rev. Lett.* **102**, 180501 (2009).
- [28] M. S. Underwood, and D. L. Feder, Universal quantum computation by discontinuous quantum walk, *Phys. Rev. A* **82**, 042304 (2010).

- [29] A. M. Childs, D. Gosset, and Z. Webb, Universal computation by multiparticle quantum walk, *Science* **339**, 791 (2013).
- [30] P. Kurzynski, and A. Wojcik, Quantum walk as a generalized measuring device, *Phys. Rev. Lett.* **110**, 200404 (2013).
- [31] P. Rebentrost, M. Mohseni, I. Kassal, S. Lloyd, and A. A. Guzik, Environment-assisted quantum transport *New J. Phys.* **11**, 033003 (2009).
(2012).
- [32] L. Sansoni, F. Sciarrino, G. Vallone, P. Mataloni, A. Crespi, R. Ramponi, and R. Osellame, Two-particle bosonic-fermionic quantum walk via integrated photonics, *Phys. Rev. Lett.* **108**, 010502 (2012).
- [33] P. Xue, R. Zhang, H. Qin, X. Zhan, Z. H. Bian, J. Li, and B. C. Sanders, Experimental quantum-walk revival with a time-dependent coin *Phys. Rev. Lett.* **114**, 140502 (2015).
- [34] B. Do, M. L. Stohler, S. Balasubramanian, D. S. Elliott, C. Eash, E. Fischbach, M. A. Fischbach, A. Mills, and B. Zwickl, Experimental realization of a quantum quincunx by use of linear optical elements, *Opt. Soc. Am. B* **22**, 020499 (2005).
- [35] H. Schimmitz, R. Matjeschk, C. Schneider, J. Glueckert, M. Enderlein, T. Huber, and T. Schaetz, Quantum walk of a trapped ion in phase space, *Phys. Rev. Lett.* **103**, 090504 (2009).
- [36] F. Zaehring, G. Kirchmair, R. Gerritsma, E. Solano, R. Blatt, and C. F. Roos, Realization of a quantum walk with one and two trapped ions, *Phys. Rev. Lett.* **104**, 100503 (2010).
- [37] M. Karski, L. Forster, J. M. Choi, A. Steffen, W. Alt, D. Meschede, and A. Widera, Quantum walk in position space with single optically trapped atoms, *Science* **325**, 174 (2009).
- [38] P. Xue, B. C. Sanders, A. Blais, and K. Lalumiere, Quantum walks on circles in phase space via superconducting circuit quantum electrodynamics, *Phys. Rev. A* **78**, 042334 (2008).
- [39] E. Flurin, V. V. Ramasesh, S. Hacohen-Gourgy, L. S. Martin, N. Y. Yao, and I. Siddiqi, Observing Topological Invariants Using Quantum Walks in Superconducting Circuits, *Phys. Rev. X* **7**, 031023 (2017).
- [40] J. Ghosh, Simulating Anderson localization via a quantum walk on a one-dimensional lattice of superconducting qubits, *Phys. Rev. A* **89**, 022309 (2014).
- [41] Y. Hirayama, A. Miranowicz, T. Ota, G. Yusa, K. Muraki, S. K. Özdemir, and N. Imoto, Nanometre-scale nuclear-spin device for quantum information processing, *J. Phys.: Condens. Matter* **18**, S885 (2006).

- [42] A. Miranowicz, S. K. Ozdemir, J. Bajer, G. Yusa, N. Imoto, Y. Hirayama, and F. Nori, Quantum state tomography of large nuclear spins in a semiconductor quantum well: Robustness against errors as quantified by condition numbers, *Phys. Rev. B* **92**, 075312 (2015).
- [43] T. Liu, S. J. Xiong, X. Z. Cao, Q. P. Su, and C. P. Yang, Efficient transfer of an arbitrary qutrit state in circuit quantum electrodynamics, *Opt. Lett.* **40**, 5602 (2015).
- [44] F. Wang, L. Yu, Q. P. Su, and C. P. Yang, Simple scheme for information transfer of a qutrit in circuit QED, *Prog. Theor. Exp. Phys.* **2017**, 073J01 (2017).
- [45] F. Yan, S. Gustavsson, A. Kamal, J. Birenbaum, A. P. Sears, D. Hover, T. J. Gudmundsen, D. Rosenberg, G. Samach, S. Weber, J. L. Yoder, T. P. Orlando, J. Clarke, A. J. Kerman, and W. D. Oliver, The flux qubit revisited to enhance coherence and reproducibility, *Nat. Comm.* **7**12964 (2016)
- [46] J. Q. You, X. D. Hu, S. Ashhab, and F. Nori, Low-decoherence flux qubit, *Phys. Rev. B* **75**, 140515(R) (2007).
- [47] M. J. Peterer, S. J. Bader, X. Y. Jin, F. Yan, A. Kamal, T. J. Gudmundsen, P. J. Leek, T. P. Orlando, W. D. Oliver, and S. Gustavsson, Coherence and decay of higher energy levels of a superconducting transmon qubit, *Phys. Rev. Lett.* **114**, 010501 (2015).
- [48] C. Rigetti, J. M. Gambetta, S. Poletto, B. L. T. Plourde, J. M. Chow, A. D. Corcoles, J. A. Smolin, S. T. Merkel, J. R. Rozen, G. A. Keefe, M. B. Rothwell, M. B. Ketchen, and M. Steffen, Superconducting qubit in a waveguide cavity with a coherence time approaching 0.1 ms, *Phys. Rev. B* **86**, 100506(R) (2012).
- [49] I. M. Pop, K. Geerlings, G. Catelani, R. J. Schoelkopf, L. I. Glazman, and M. H. Devoret, Coherent suppression of electromagnetic dissipation due to superconducting quasiparticles, *Nature* **508**, 369 (2014).
- [50] W. Chen, D. A. Bennett, V. Patel, and J. E. Lukens, Substrate and process dependent losses in superconducting thin film resonators, *Sci. Technol.* **21**, 075013 (2008).
- [51] P. J. Leek, M. Baur, J. M. Fink, R. Bianchetti, L. Steffen, S. Filipp, and A. Wallraff, Cavity quantum electrodynamics with separate photon storage and qubit readout modes, *Phys. Rev. Lett.* **104**, 100504 (2010).
- [52] M. Baur, S. Filipp, R. Bianchetti, J. M. Fink, M. Goppl, L. Steffen, P. J. Leek, A. Blais, and A. Wallraff, Measurement of Autler-Townes and Mollow Transitions in a Strongly Driven Superconducting Qubit, *Phys. Rev. Lett.* **102**, 243602 (2009).